

Jia'en Lin *Editor*

# Proceedings of the 2021 International Petroleum and Petrochemical Technology Conference

 Springer

# Proceedings of the 2021 International Petroleum and Petrochemical Technology Conference

Jia'en Lin  
Editor

# Proceedings of the 2021 International Petroleum and Petrochemical Technology Conference

*Editor*

Jia'en Lin

College of Petroleum Engineering

Xi'an Shiyou University

Xi'an, Shaanxi, China

ISBN 978-981-16-9426-4

ISBN 978-981-16-9427-1 (eBook)

<https://doi.org/10.1007/978-981-16-9427-1>

© The Editor(s) (if applicable) and The Author(s), under exclusive license to Springer Nature Singapore Pte Ltd. 2022

This work is subject to copyright. All rights are solely and exclusively licensed by the Publisher, whether the whole or part of the material is concerned, specifically the rights of translation, reprinting, reuse of illustrations, recitation, broadcasting, reproduction on microfilms or in any other physical way, and transmission or information storage and retrieval, electronic adaptation, computer software, or by similar or dissimilar methodology now known or hereafter developed.

The use of general descriptive names, registered names, trademarks, service marks, etc. in this publication does not imply, even in the absence of a specific statement, that such names are exempt from the relevant protective laws and regulations and therefore free for general use.

The publisher, the authors and the editors are safe to assume that the advice and information in this book are believed to be true and accurate at the date of publication. Neither the publisher nor the authors or the editors give a warranty, expressed or implied, with respect to the material contained herein or for any errors or omissions that may have been made. The publisher remains neutral with regard to jurisdictional claims in published maps and institutional affiliations.

This Springer imprint is published by the registered company Springer Nature Singapore Pte Ltd. The registered company address is: 152 Beach Road, #21-01/04 Gateway East, Singapore 189721, Singapore

# Contents

## **Static and Dynamic Reservoir Evaluation and Management in E&P**

<b>Application of Prestack Wide-Azimuth Coherence Technique in Complex Fault Area</b> . . . . .	3
Min Xu, Jing Luo, Hong Liang, Rong-rong Yang, Ying Deng, Fan Yang, Yue-zong Zhou, and Li-feng Gao	
<b>Multiple Hydraulic Fractured Vertical Wells in Gas Condensate Reservoirs</b> . . . . .	13
Abdollah Esmaceli, Yermek Aubakirov, and Kanapiyeva Fatima Mukhidinovna	
<b>A Systemic Study on Production Index Behavior of Earlier Polymer Flood in Offshore Heterogeneous Heavy-Oil Reservoirs</b> . . . . .	28
Zhi-jie Wei, Xiao-dong Kang, Han-xu Yang, and Yu-yang Liu	
<b>Determination of Surfactant Concentration in Surfactant-polymer Mixtures for Improving Oil Production</b> . . . . .	39
Jian Hou, Ming Han, Abdulaziz Alkateeb, and Abdulkareem Alsofi	
<b>Study of Preformed Particle Gel Blocking Performance in Fractured Carbonate Reservoirs</b> . . . . .	50
Dong-qing Cao, Ayman Almohsin, Ming Han, and Bader Al-Harbi	
<b>Failure Behaviour Simulation of Shale Layer Under Brazilian Test with Particle Flow Code</b> . . . . .	67
Bo Liu, Wei Huang, Feng Sun, Bing-bing Zhao, and Shi-feng Xue	
<b>Research on Profile Control and Flooding Effect Evaluation of Horizontal Wells on the Basis of Improved Hall Curve</b> . . . . .	77
Li-jian Zhang, Pan-pan Tian, Yan-jun Yin, Yi-wei Ren, and Zhen Zhang	

<b>Geological Modeling Method and Application of Rapid Facies Transition Sand Bodies in Tidal-Controlled Delta . . . . .</b>	<b>85</b>
Zhou Lyu, Shengen Gao, Shu-dai Peng, and Yu-kun Lan	
<b>Study on Pore Shape and Pore Size Distribution of Carbonate Reservoir with Complex Pore Structure in Dengying Formation, Sichuan Basin . . . . .</b>	<b>93</b>
Dan Zhao, Li Wang, Zhi-jin Pu, Chang-hong Cai, Jue-dong An, and Man-fei Chen	
<b>Classification and Undiscovered Resource Assessment of Oil and Gas Bearing Basins in South America . . . . .</b>	<b>109</b>
Hai-guang Bian, Zhi-xin Wen, and Cheng-peng Song	
<b>Development Characteristics and Main Controlling Factors of Tidal Sand Bar in Estuary . . . . .</b>	<b>118</b>
Ke-xin Zhang, Ming-ming Tang, Chao-qian Zhang, Xue-peng Wan, Hong Huo, Jun-chang Wu, Zheng Meng, Yu-sheng Wang, Tian-jian Sun, and Di Han	
<b>Application of Tracer Monitoring Technology in Production Wells . . . .</b>	<b>128</b>
Ying Zhang, Jun-liang Li, Yong-quan Xu, Jing Cheng, and Jin-jian Yao	
<b>Stress Analysis of Premium Tubing Connection with Different Make-Up Torque in Different Well Depth . . . . .</b>	<b>136</b>
Yang Yu, Yin-ping Cao, Fang-ting Hu, Mao-xian Xiong, and Yi-hua Dou	
<b>Recent Advances in Metallic Honeycomb Structure . . . . .</b>	<b>144</b>
Ya-fei Zhang, Jing-wei Liang, Hong-tao Liu, Hong-xue Mi, and Yi-hua Dou	
<b>Neuro-Fuzzy Approach for Gas Compressibility Factor Prediction . . . .</b>	<b>157</b>
A. Abelrigeeb Al-Gathe, Abbas M. Al-Khudafi, Abdulrahman Al-Fakih, and A. A. Al-Wahbi	
<b>Finely Description for Fractured Reservoir and Comprehensive Evaluation of Seismic . . . . .</b>	<b>166</b>
Jing Luo, Xiao Yang, Lan-ying Wang, Xiao Li, Min Xu, Hai-yang Guo, Zheng Wang, and Wei Deng	
<b>Application of Rock Typing in Static and Dynamic Reservoir Characterization . . . . .</b>	<b>174</b>
Hassan Aharipour and Fatemeh Sadat Masoumi	

<b>Inferences Derived from Reservoir Permeability Estimation Using Static and Dynamic Data: Core Data Analysis Versus Drawdown Tests . . . . .</b>	<b>184</b>
Francis Nwabia, Jude Osamor, Robinson Madu, Nkemakolam Izuwa, and Anthony Chikwe	
<b>Study and Application of Horizontal Well Enhanced Oil Recovery Technology on Huabei Oilfield Jin45 Fault Block . . . . .</b>	<b>197</b>
Xin Wang, Ning Li, Changjun Long, Mengmeng Ning, Zhengdong Xu, Jiangfen Jia, Jianchao Tian, Mengmei Xiao, Weizhong Kong, Qilun Liu, Hongxin Huo, and Yongguang Chen	
<b>The Development and Application of Rotatable Universal Wireline Adapter . . . . .</b>	<b>206</b>
Hua-qing Zhang, Yan-sheng Song, Xian-bao Li, Guo-jiang Yu, and Wei-quan Li	
<b>Evaluation of Stratigraphic and Reservoir Sand Continuity Across Two Fields in Niger Delta Basin Using Seismic, Well Log, Core and Biostratigraphic Data . . . . .</b>	<b>215</b>
Robinson O. Madu, Charles C. Ugbor, and Francis N. Nwabia	
<b>Magnetic-Thermal-Fluid Field Coupling Method Study on Temperature Rise Analysis of Permanent Magnet Motor . . . . .</b>	<b>223</b>
Li-ping Tan, Yu-fu Zhou, Wen-sheng Xiao, Jun-guo Cui, Hai-Yang Zhao, Hao-zhi Qin, Lian-peng Mei, Chang-jiang Li, and Xiang Gao	
<b>Drilling, Production</b>	
<b>Application and Analysis of Precisely Controlled Corresponding Fracturing Technology in Thin-Poor Layers of D Oilfield-Take A Well Group in X Region for Example . . . . .</b>	<b>235</b>
Xun Li	
<b>Main Evaluation Factors of Fractured Formation Leakage in Bohai Bay Basin . . . . .</b>	<b>246</b>
Shao-long Jiang, Guo-qiang Zhang, Gui-peng Mu, Ren-guo Yuan, and Zhao-ling Xin	
<b>Living Polymer with Special Functional Groups to Displace Oil and Control Profile in Thin and Poor Layers . . . . .</b>	<b>258</b>
Zhi-hui Sun	
<b>Research and Field Application of Injection-Production Stratified Process Pipe String Technology for Screw Pump Wells in the Same Well . . . . .</b>	<b>266</b>
De-kui Xu, Chong-jiang Liu, Fei Yao, Yu-chuan Liu, and Bai-tao Ma	

<b>Study on Optimization Method of Structural Parameters About Jetting and Helical Combination Drain Tool . . . . .</b>	<b>275</b>
Huanle Liu and Shifeng Xue	
<b>Mechanism Analysis of Nano-magnetic Fluid Displacing Crude Oil . . . .</b>	<b>290</b>
Guan-zheng Qu, Jian Su, and Peng Jiao	
<b>Study on Optimization of Plugging Position for Temporary Plugging and Diverting Fracturing . . . . .</b>	<b>297</b>
Xu Wei	
<b>Application Research of Tracer Monitoring Technology After Fracturing in Horizontal Well . . . . .</b>	<b>307</b>
Dawei Deng, Pengfei Tang, Xu Wei, Dezha Zhao, and Shilu Wang	
<b>Evaluation of the Effects of Nano-asphalt on Drilling Mud Properties and Its Impact Shale Stability . . . . .</b>	<b>314</b>
Zhao Xionghu, Egwu Saviour Bassey, and Deng Jingen	
<b>Analysis of Historical Production Data for Reservoir Performance Prediction of X Oil Field . . . . .</b>	<b>326</b>
Mohamed Yasser Mohamed Sabri Farag Eita and Elhassan Mostafa Abdalla Mohammed	
<b>Estimation of Bottom-Hole Temperature Based on Machine/Deep Learning . . . . .</b>	<b>340</b>
Abdulrahman Al-Fakih and KeWen Li	
<b>Fishbone Technology for Completing Unconventional Reservoir . . . . .</b>	<b>354</b>
Chinedu Ejike and Tian Shouceng	
<b>Operations and Equipment of Well Drilling . . . . .</b>	<b>361</b>
Mohammed Raed Al-Sheikh Jadeer	
<b>Analysis and Investigation of the Effects of Particle Size and Concentration on Sand Screen Erosion Prediction and Modelling . . . . .</b>	<b>367</b>
Abdullah Abduljabbar, Mysara Mohyaldinn, and Ahmed Alghurabi	
<b>The Movement and Force Analysis of Temporary Plugging Ball for Perforated Holes in Directional Well . . . . .</b>	<b>383</b>
He-wen Zhang, Hong-lan Zou, An-le He, Chong Liang, Hong-ge Jia, Hong-hua Zhou, and Shun-xiang Gong	
<b>Discussion on Artificial Intelligence Oil Production Technology of Rod Pumped Well . . . . .</b>	<b>390</b>
Yan-hui Zhu, Peng Gao, Liang-liang Qiu, Juan-juan Yan, Yu Han, Peng-gang Chang, and Wen-mao Liu	
<b>Study on Cross Layer Plugging Technology for Injection Well . . . . .</b>	<b>400</b>
Lin Zhongchao, Sun Jiang, Zhao Xuyang, Han Xiaohui, and Huang Ming	



<b>Research and Practice of Integrity Evaluation Technology for Deep Gas Wells</b> .....	409
Wei-ming Huang, Nan Zhang, Zhi-bo An, Peng Wang, and Wei Liu	
<b>An Intelligence ROP Optimization Method for Horizontal Well Drilling</b> .....	419
Cheng Zhong, Li Ning, and Ding Xiang-xiang	
<b>Research and Application of Downhole Oil-Water Separation and Injection Production Technology in the Same Well</b> .....	427
Guo-xing Zheng, Meng Cai, Wei-wei Li, Yong-gang Peng, and Guang-ling Zhou	
<b>Local Materials Drilling Mud: A Laboratory Approach</b> .....	436
Azam Khan and Ameer Hamza	
<b>Evaluation of Dry Friction Reducers for Slickwater Fracturing at an Elevated Temperature</b> .....	442
Ziyuan Qi, Ming Han, Mohammed Bataweel, and Jose I. Rueda	
<b>Research and Application of Adaptive Control Method for Managed Pressure Drilling</b> .....	451
Qi-jun Wang, Zhi-gang He, Fa-ming Lu, and Xue-gang Li	
<b>Development and Application of Foam Generator for Low Pressure Loose Sandstone Gas Well</b> .....	459
Zhi-xuan Zhang, Ting-chao Yan, Ming-chun Lu, Meng-long Zhao, Yan-ping Liu, Bai-Jie, and Chang-ping Gong	
<b>Oil and Gas Storage and Transportation and Flow Assurance</b>	
<b>Analysis of Remaining Strength and Failure of Submarine Pipeline with Double-Point Corrosion Defects</b> .....	475
Zhuo-yu Fang, Shao-hua Dong, and Yu-hang Duan	
<b>Brief Analysis of New Lightning Current Detection Technology for Oil Tank</b> .....	491
Si-Xue Chen, Yi-Ying Zou, and Ren-Jie Lou	
<b>An Optimized Design of Jet Pig Used for Gas Pipeline Pigging</b> .....	501
Dong-liang Yu, Yu-ting Liu, Yi Jiang, Lei-chao Wang, and Dong-hua Peng	
<b>Research on On-line Nondestructive Testing Method of Pipeline Erosion Based on Electromagnetic Field</b> .....	516
Qi-jun Wang, Ming-sheng Li, Yong Yu, and Kun Xiao	

<b>Effect of Cyclone on Purification and Separation Performance of Supersonic Separator</b> . . . . .	527
Jia-nan Chen, Wen-ming Jiang, Ce Wang, and Chao Li	
<b>Low Concentration Surfactant and Polymer Formulations for SP Injection at HTHS Condition</b> . . . . .	540
Jian Hou, Ming Han, Ziyad Kaidar, and Abdulkareem Alsofi	
<b>Study on Particle Erosion Prediction of Elbows and Plugged Tees in Gas-Solid Flow</b> . . . . .	548
Xiang-yang Zhao, Xue-wen Cao, Heng-guang Cao, Zhen-qiang Xie, Ni Xiong, and Chao Wu	
<b>Study and Application of Gathering and Transportation Limit at Low Temperature of Produced Fluid in Huabei Oilfield</b> . . . . .	566
Tao Lin, Hong-song Gao, Shu-hua Zhao, Kang Zeng, Feng Gong, and Wei Yang	
<b>Mixture Design of Solvent for CO<sub>2</sub>-C<sub>2</sub>H<sub>6</sub> Azeotrope in Extractive Distillation</b> . . . . .	581
Hai-qin Wang, Ce Wang, Zu-bin Zhang, Feng-qi Li, and Xiao-dong Yan	
<b>Sand Erosion in Subsurface and Surface Oil Production Components</b> . . . . .	596
Mysara Mohyaldinn and Abdullah Abduljabbar	
<b>Research on Monitoring Method of Seal Leakage of Pumps Based on Image Recognition</b> . . . . .	605
Wencai Liu, Zhijie Gao, Yingli Li, and Minhui Zhang	
<b>Intelligence and Information Technology</b>	
<b>Theoretical Study of In-phase Forwarding in Enhancing Underground Wireless Electromagnetic Relay Transmission</b> . . . . .	623
Wan-jiang Wang, Wei-qin Li, Chang-min Liu, Yu-han Wu, Lei Lin, Meng Peng, and Hon-fei Tan	
<b>Feasibility Study on Recognition of Large Reservoir Fractures by Cross-Well Electromagnetic Detection Based on Neural Network</b> . . . . .	639
Yu-han Wu, Wei-qin Li, Chang-min Liu, Wan-jiang Wang, Lei Lin, and Meng Peng	
<b>Design and Implementation of Drilling Parameter Acquisition System Based on “Simulation Mode”</b> . . . . .	653
Sheng-wa Liu and Yong Dai	
<b>Prediction of Octane Number Loss and Parameter Optimization in Gasoline Refining Process</b> . . . . .	660
Hao-ling Huo, Qing-ding Wu, Min Zou, and Zen-nan Xu	

<b>Application of the Fourth-Generation Injection and Dynamic Monitoring Technology in Huabei Oilfield . . . . .</b>	<b>670</b>
Peng-wei Li, Tao Ji, Hong-lin Luo, Xu Zhang, Wei-ang Li, Jing Zuo, and Jian-ning Wang	
<b>Exploration and Research on Intelligent Maritime Safety Management for Offshore Oil in New Circumstances . . . . .</b>	<b>682</b>
Feng Tao, Yan-ming Teng, and Xue-hui Li	
<b>A New Method for Geochemical Prediction of the Existence of Petroleum Reservoirs in Magmatic and Metamorphic Rocks . . . . .</b>	<b>694</b>
Adil Ozdemir and Yildiray Palabiyik	
<b>Reliability in Sociotechnical Systems for the Risky Industry: Cases from Chemical Process Industries . . . . .</b>	<b>703</b>
Salvador Ávila Filho and Lucas Menezes Pereira	
<b>Study on Application of Relief Well Guidance Based on Fully Connected Network . . . . .</b>	<b>716</b>
Chang-min Liu, Wei-qin Li, Wan-jiang Wang, Yu-han Wu, Lei Lin, and Meng Peng	
<b>Generating Indicator Diagram of Pumping Well with Electric Power Data Based on Deep Learning . . . . .</b>	<b>726</b>
Zhan-min Zhang, Yu-fang Liu, Fei Cao, Li-hong Du, Gui-zhi Min, Li Hao, and Xue-min Bai	
<b>Study on Prediction Method of Water Injection Profile Based on XGBoost algorithm . . . . .</b>	<b>738</b>
Ya-xuan Wang, Jian-wei Gu, Zhi-yong Wei, and Hong-bo Liu	
<b>Simulation Match of the Sudan Jake-S Oilfield Production History . . . .</b>	<b>752</b>
Sheikh Tawil Abdalhalim Yosri, Xiao-juan Lai, Lei Wang, and Mukhtar Yasir	
<b>Development of AI Tools for Engineering: Advantages versus Ethical Dilemmas . . . . .</b>	<b>762</b>
Hamed Z. Qadim	
<b>Author Index . . . . .</b>	<b>773</b>

# **Static and Dynamic Reservoir Evaluation and Management in E&P**



# Application of Prestack Wide-Azimuth Coherence Technique in Complex Fault Area

Min Xu<sup>1</sup>(✉), Jing Luo<sup>1</sup>, Hong Liang<sup>1</sup>, Rong-rong Yang<sup>1</sup>, Ying Deng<sup>1</sup>, Fan Yang<sup>1</sup>,  
Yue-zong Zhou<sup>1</sup>, and Li-feng Gao<sup>2</sup>

<sup>1</sup> BGP Southwest Geophysical Research Institute, Chengdu, China  
xumin\_sc@cnpc.com.cn

<sup>2</sup> The Second Geophysical Prospecting Company of Daqing, BGP.INC.CNPC, Songyuan, China

**Abstract.** The Permian in the northwest of Sichuan Basin is buried deep (more than 6000 m), and a large number of small Fault Horst structures are developed. The fracture system is very well developed, which leads to multiple solutions of prediction results, and the effect of various prediction techniques is very poor. Using the characteristics that P-wave propagates in parallel or vertical fractures in anisotropic media, the properties of seismic reflection data are studied, and the seismic information is mined to guide the study of fracture development law. Based on the seismic data of “two widths and one height”, the prestack wide-azimuth coherent fracture prediction technology is studied. First of all, according to the post stack coherent attributes to find the general law of fault system development, then, the wide-azimuth data are divided into azimuth and angle. On the partial stack data volume with azimuth, the azimuth coherence volume is calculated by using the characteristics of seismic amplitude changing with azimuth, so as to predict the development characteristics of faults and fractures.

Prestack wide-azimuth coherence technique is more close to the actual geological phenomenon in describing the fault development zone and the morphological characteristics of fault and fracture cavity, which is helpful to the selection of drilling well location target. Compared with the conventional post stack coherence technology, it not only reduces the multi solution, but also can predict relatively small-scale fractures. At the same time, it has the anti-interference ability of post stack coherence, and has the characteristics of fast and efficient prediction, which is suitable for rapid and efficient exploration and development stage.

**Keywords:** Wide-azimuth · Fault system · Fracture prediction · Azimuth · Coherence

## 1 Introduction

The study area is located in the footwall of the nappe structural belt of LM Mountain Piedmont belt in the northwest of Sichuan Basin (Fig. 1). Affected by structure of many times activity, the hinterland structural fold has a huge range, which is a fault fold belt with developed faults, and the small faults are very developed. The buried depth of the

Permian Maokou Formation is more than 6000 m. The overlying strata and the underlying strata have a large set of kneading gypsum strata. There are few upward and downward faults, and a large number of small fault Horst structures are developed (Fig. 2). The lithology is mainly marine carbonate rocks, and a large number of dissolution pores and fractures are the effective space for oil and gas accumulation. According to the analysis of drilling results, the main reservoir type is fractured-porosity type. Fracture is the main channel and reservoir, which is one of the main factors for high production. The corrosion holes and fractures can be seen on the electrical imaging logging map. The fracture strike is mainly NW-SE, the dip angle changes greatly, and the local fracture is mainly medium high angle fracture.

Because the resolution of seismic exploration is only a few meters to tens of meters, it is easy to detect the fracture cave system or development zone composed of many small fractures and caves, but it is unable to identify single or small fractures and caves. A variety of fracture prediction techniques have also been studied in this area. However, with the increase and acceleration of exploration and development, the requirements for fracture prediction are higher and higher. The limitations of seismic data obtained by conventional seismic exploration are gradually obvious, especially the problems of narrow azimuth and low spatial resolution, which seriously affect the identification of fractured vuggy gas reservoirs in this area. Prestack fracture detection technology can detect high angle fracture development zone, and exploring a new fast high-resolution fracture prediction technology based on prestack seismic data is the key to the study area.

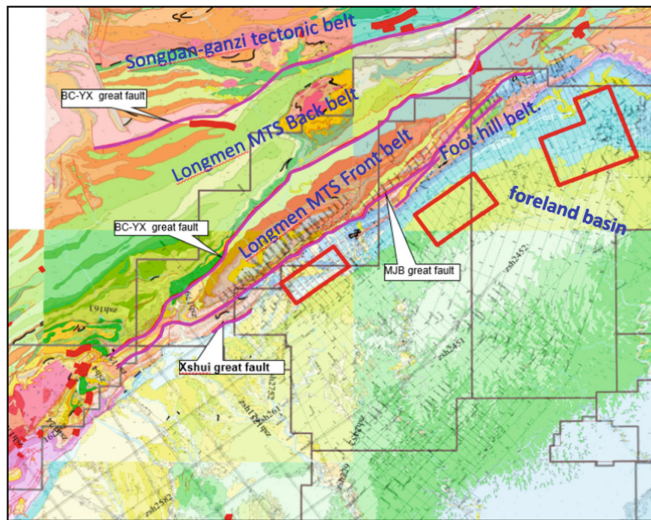


**Fig. 1.** Geological plan of study area.

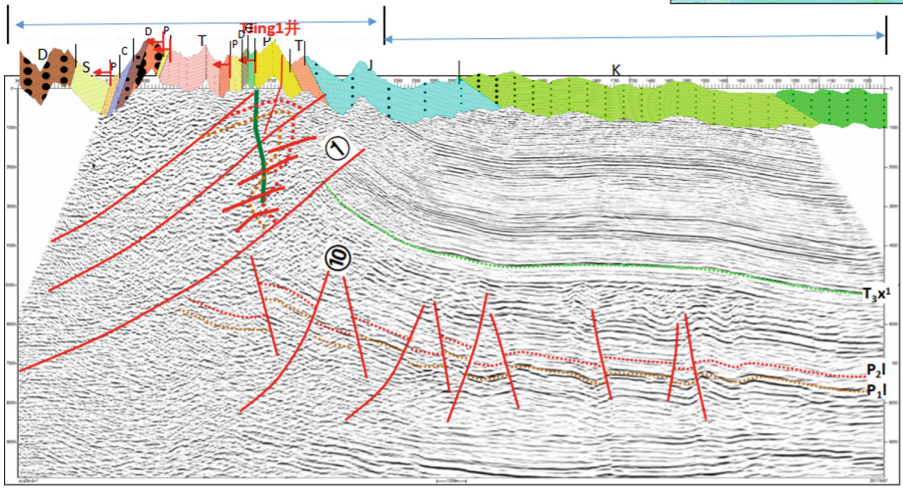


Fig. 2. Seismic section.

## 2 Prestack Wide-Azimuth Coherence Cube Technique

### 2.1 Principle of Prestack Wide-Azimuth Coherence Cube Technique

This method can predict relatively small-scale fractures by using the characteristics of seismic amplitude changing with azimuth, which provides a new idea and method for fracture detection and reservoir prediction.

Coherence technology is a technology that uses correlation principle to highlight the non similarity of seismic signals between adjacent traces, so as to detect faults and reflect the distribution of geological anomaly characteristics. According to the spatial variation of high and low coherence values, faults can be identified quickly, even small faults and small distortions that are difficult to be identified in conventional interpretation can be identified. Therefore, the magnitude of signal coherence between seismic traces is an important indicator to judge the existence of faults or fractures [1–4]. The stronger the coherence, the more continuous the formation.

Wide-azimuth data refers to the seismic data obtained by wide-azimuth seismic exploration acquisition technology. Because of the full azimuth distribution, reasonable offset and coverage times distribution, it is more conducive to the correct imaging of complex geological bodies in underground structure, and has high resolution. wide-azimuth seismic data contains more abundant information, which is helpful to identify micro structures, small faults and high angle fractures. Therefore, more seismic attribute information can be obtained by using wide-azimuth data for fracture detection in deep structural complex areas.

Wide-azimuth coherency is that the wide-azimuth data is stacked by azimuth, and then the coherence calculation is realized based on the characteristics of amplitude changing with azimuth on the azimuth data volume. It is based on the discontinuous information changing with spatial azimuth, which eliminates the multi solution caused by lithology change, and can also predict the small-scale fracture development zone.

However, the post stack coherent fracture prediction technology in conventional oil and gas exploration is only based on the reflection amplitude difference between each point in space and the surrounding points, which can not avoid the waveform change caused by lithology change. The schematic diagram of the two is shown in Fig. 3.

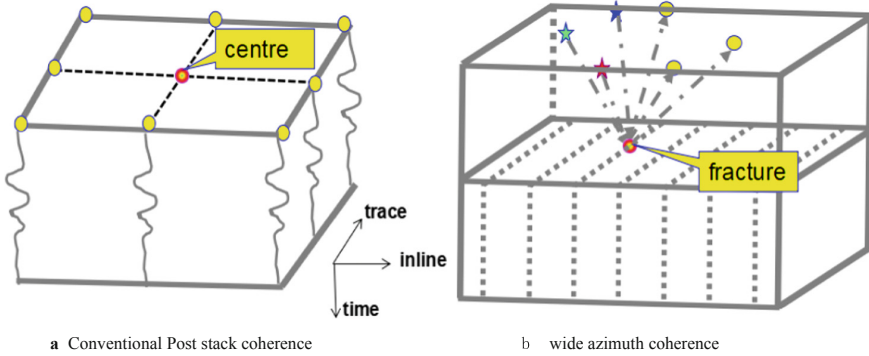


**Fig. 3.** Difference between conventional coherence and wide-azimuth coherence.

## 2.2 Prestack Wide-Azimuth Coherent Calculation Flow (Algorithm and Flow)

Compared with conventional post stack coherence, the wide-azimuth high-precision coherence technology increases the azimuth processing of seismic data first, which reduces the multi solution of prediction, and can predict relatively small-scale fractures, so as to realize the synchronization of large-scale and small-scale fractures, and the accuracy is higher.

The calculation process of wide-azimuth coherence technique is as follows:

- 1) Read  $N$  original wide-azimuth seismic data ( $n$  is greater than or equal to 3);
- 2) Construction of covariance matrix: according to the inline and Xline cycles, taking a certain time point of the seismic data as the center of the sliding time window, take out the seismic trace data with the length of the coherent time window, construct the matrix trace of 6 times the length of the coherent time window, and then multiply the transpose of the matrix trace by the matrix trace to obtain the covariance matrix  $C$ .
- 3) The covariance matrix  $C$  is decomposed into eigenvalues, and the maximum eigenvalue is divided by the sum of all eigenvalues to get the coherence value of the point. The algorithm flow is shown in Fig. 4.

Combined with logging and forward modeling information, on the basis of logging data calibration, for the same grid, the dissolution holes and fractures are merged into a geometric structure geological model. Through the production dynamic data, the wave impedance/porosity threshold value is determined to filter the surrounding rock, and finally the effective three-dimensional geometric structure model is obtained. On this



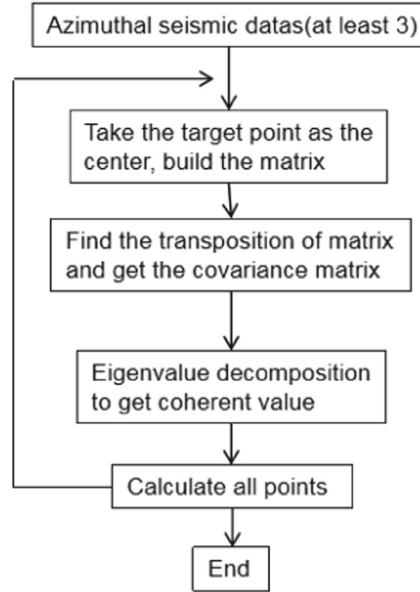


**Fig. 4.** Wide-azimuth and high precision coherent flow chart.

basis, the fracture cavity zone/system/unit division analysis can be carried out in combination with the production dynamic data. In addition, when merging, the threshold fusion method can be used to carry out the comprehensive prediction of fractures and holes, and then the 3D carving based on the boundary constraints can be carried out to study the development of fractures and holes.

### 2.3 Characteristics and Key Technologies of Wide-Azimuth Coherence Cube

Wide-azimuth coherence technology is based on wide-azimuth data volume, introduces the traditional coherence calculation method, and then realizes high-precision coherence attribute calculation. The key technology is the azimuth division of wide-azimuth seismic data. The principle is to effectively meet the uniform coverage times of each azimuth, which can effectively improve the fracture identification. The basis of division is to extract coherence slice from post-stack seismic data or along layer coherence attribute, find the general orientation of fault system and fracture development in the study area [5, 6], and then stack the divided gather data; the second is to select the time point of seismic data and the time window length when constructing the covariance matrix, and determine the time window according to the general reflection time of the target horizon. The time window is too long, it contains many in-phase axes, the coherence volume can not accurately reflect the characteristics of the fault; the time window is too small, it can not contain a complete waveform, the coherence volume data is unreliable, usually greater than  $t/2$  and less than  $3t/2$ ,  $t$  is the period of seismic wave reflection; finally, the eigenvalue decomposition, select the eigenvalue representing fracture development,

remove the noise interference eigenvalue, can be used in order to improve the resolution of coherent volume calculation.

3 Application Effect Analysis

Well ST1, well ST3 and well SY001-X1 in the study area have achieved high production, and the fracture cavity is of great significance for the improvement of reservoir. In the study area, “two wide and one high” (wide-azimuth, wide frequency band, high density) high-precision seismic acquisition technology (the number of coverage is 10 \* 10, and the transverse longitudinal ratio is 0.85) is used to obtain seismic data. The wide-band signal source and vibroseis can obtain more azimuth information, which can realize the flexible division of azimuth and provide reliable seismic data for fine fracture prediction.

The prestack wide-azimuth coherence technique is used to study the fractures in this area. The main processing flow of pre-stack fracture detection is dividing azimuth, and the general direction of fracture azimuth in the study area can be found from the post stack coherent slices. The study area is cut by many NE trending faults, which are obviously controlled by faults. The structures are long strip-shaped anticline, fault anticline, a small number of fault nose and fault block structures in NE direction. The fault system is distributed in NE direction, and the fractures are mainly developed along the direction of the fault system. However, there are many groups of fractures in multiple directions between the major fault systems (Fig. 5), so the fractures are fully considered in order to improve the identification ability of fractures and meet the principle of uniform coverage times in each direction, six directions are divided (Table 1).

Table1. Azimuth division.

Central azimuth (°)	6	36	66	96	126	156
Azimuth range (°)	−9–21	21–51	51–81	81–111	111–141	141–171

Omni directional angle domain imaging is a full wave field multi-path migration imaging technology based on ray theory. In different azimuth migration profiles, the anisotropy characteristics of fracture development are obvious [7–9]. From the section (Fig. 6), the characteristics of seismic reflection waves in various directions are similar, but more different. The blue arrow mark is about 10–20 ms down from the top boundary of Maokou Formation, indicating the position of fracture development section. When extracting the wide-azimuth coherent attribute, the window is set as 20 ms down from the target horizon. Through the analysis of different azimuthal stack sections, it is found that the energy of in-phase axis changes at different azimuths, showing strong anisotropy. The characterization of fractures on stack sections of 51°–81°, 81°–111° and 111°–141° is clearer. Therefore, the coherence attribute analysis is selected on these three stack sections to predict the distribution characteristics of fractures in the study area.

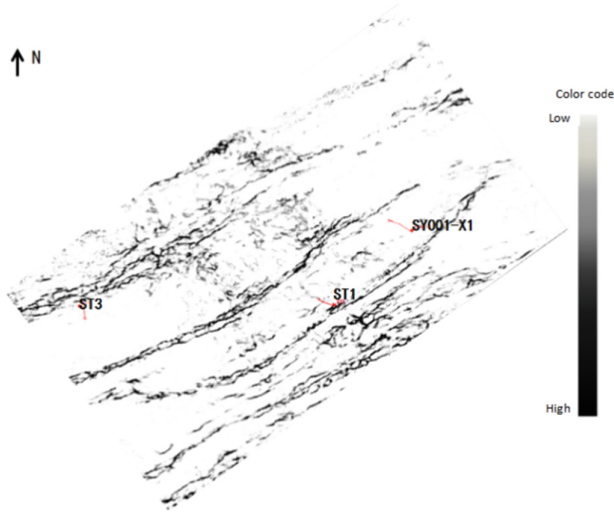


Fig. 5. Post stack coherence slice.

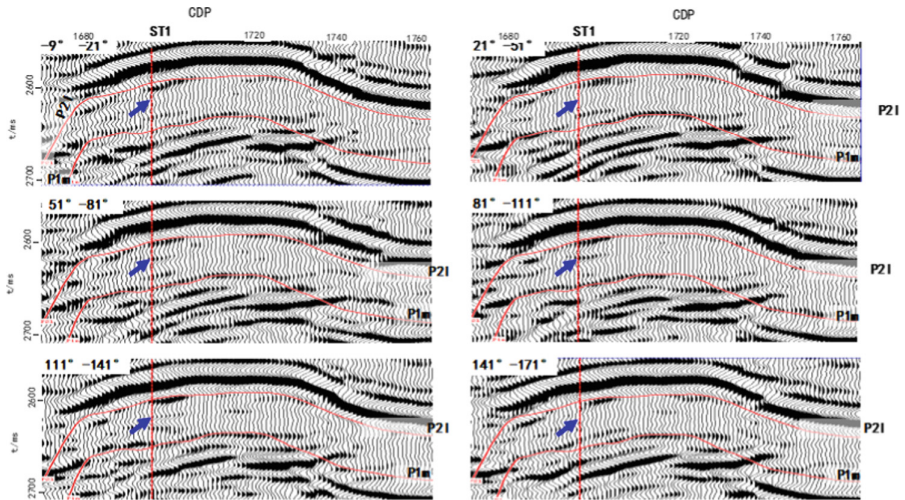
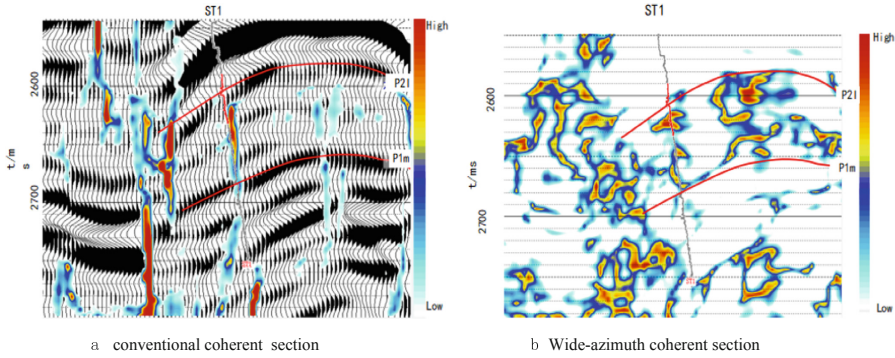


Fig. 6. Different azimuth migration sections.

On the basis of optimizing azimuth migration data, seismic attribute analysis is carried out. It can depict large-scale fractures, but there are multiple solutions [10–12]. For example, in the lower Maokou Formation, there is obvious high coherence anomaly along the track of well ST1 in conventional coherence, but in fact, the anomaly is only caused by the waveform change caused by the change of sedimentary environment, not the fault. The wide-azimuth coherence has a certain ability to depict large-scale faults and microfractures, and can better characterize the azimuth anisotropy (Fig. 7). In Maokou Formation, there are two microfractures along the well trajectory of well ST1, which

correspond to each other on the anisotropic section. Well ST1 obviously encounters microfracture development zone, which is consistent with the actual drilling and logging results. In addition, the fracture zone on the left side of well ST1 is characterized by high coherence and disordered anomaly on conventional coherence section, but different on wide-azimuth coherence section. The characterization of fracture zone by wide-azimuth coherence is consistent with the actual seismic data, and more consistent with the geological characteristics of small fault barrier development in this area.



**Fig. 7.** Comparison of conventional and wide azimuth coherence sections.

By extracting the 10 ms wide-azimuth coherence slice downward from the top boundary of Maokou Formation and superposing with fault interpretation, it can be found (Fig. 8) that there is a certain associated relationship between microfracture and fault.

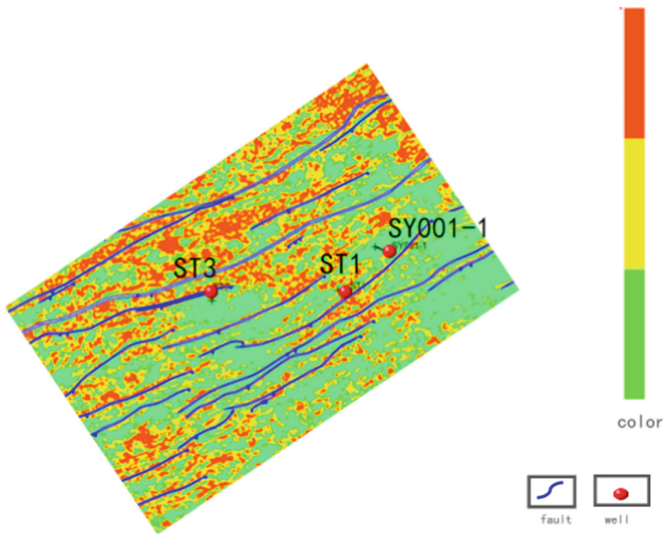


**Fig. 8.** Wide-azimuth coherent slice and fault superposition plan.

In the middle and north part of the work area (north of well ST1), microfracture is relatively more developed, and the northern structural position is relatively high, which is a favorable area for oil and gas exploration. In the later drilling, well ST3 encountered fractures and obtained more than  $80 \times 10^4 \text{ m}^3/\text{d}$  of industrial gas. The reliability of the results has been proved.

## 4 Conclusion

- 1) The wide-azimuth seismic data can provide more azimuth information and realize the flexible division of azimuth. On this basis, the azimuth coherent technology can carry out the fine prediction of fractures.
- 2) The coherence attribute based on wide-azimuth seismic data is closer to the actual geological phenomenon in describing fault development zone and fracture cavity morphology, which is helpful to the selection of drilling well location target.
- 3) The waveform discontinuity of different azimuth migration data indicates the anisotropy of azimuth. The wide-azimuth coherence technology combines the advantages of strong ability of anti-noise and high efficiency of post stack coherence technique, and has the characteristics of low multi-resolution pre-stack fracture prediction technology. It can simultaneously predict multi-scale fractures, and realize the rapid and efficient geophysical exploration ability.

**Acknowledgments.** The project is supported by Major science and technology projects of CNPC (Number 2016E-0603).

## References

1. Marfurt, K.: Kirlin RL:3-D seismic attributes using a semblance-based coherence algorithm. *Geophysics* **63**(4), 1150–1176 (1998)
2. Bahorich, M., Farmer, S.: 3-D seismic discontinuity for fault and stratigraphic features: the coherence cube. *Lead. Edge* **14**(10), 1053–1058 (1995)
3. Zhang, S., Zhang, S., Wan, G.: Available approach to structural fracture estimating—a case study of Dongying formation in eastern limb of north dagang structural zone. *Explor. Tech.* **3**(2), 38–43 (2012)
4. Watts, R.: Objectives of the US DOE 's research. *Lead. Edge* **15**(8), 906–906 (1996)
5. Li, Z., Li, Q.: Research on non-linear prediction of fracture of Oil/gas reservoir and its application. *OGP* **38**(1), 48–52 (2003)
6. Gray, D., et al.: Recent advances in determination of fracture strike and crack density from P-wave seismic data. *Lead. Edge* **21**(3), 280–285 (2002)
7. Li, M., Li, S., Zhao, Y.: The study of fractured carbonate reservoir prediction in an area in Tarim Basin. *Geophys. Prospect. Pet.* **50**(5), 24–35 (2011)
8. Huang, H., Hu, G., He, Z., Huang, D.: Carbonate fracture research using multi-scale boundary detection method. *Comput. Tech. Geophys. Geochem. Explor.* **22**(1), 21–25 (2000)
9. Wang, J., Zheng, D., Li, X., et al.: The fracture-cavern system prediction method and its application in carbonate fractured-vuggy reservoirs. *Geophys. Prospect. Pet.* **53**(6), 727–736 (2014)

10. Cao, J., He, Z., Huang, D., Li, Q.: Seismic responses to fractured reservoirs by physical modeling. *Progr. Explor. Geophys.* **26**(2), 88–93 (2003)
11. Wen, X., He, Z., Huang, D.: Application of avelet multi-scale product in fracture detection. *J. Jilin Univ. (Earth Sci. Edn.)* **38**(4), 703–707 (2008)
12. Liu, C.: Wide Azimuth seismic technology and subtle reservoir exploration. *Geophys. Prospect. Pet.* **51**(2), 138–144 (2012)



# Multiple Hydraulic Fractured Vertical Wells in Gas Condensate Reservoirs

Abdollah Esmaeili<sup>✉</sup>, Yermek Aubakirov, and Kanapiyeva Fatima Mukhidinovna

Al-Farabi Kazakh National University, Almaty, Kazakhstan

esmailyabdollah@gmail.com, miral.64@mail.ru, fatima31@mail.ru

**Abstract.** Gas reservoirs can be classified into dry gas reservoirs, wet gas reservoirs and Gas condensate reservoirs. In gas condensate reservoirs, the reservoir temperature lies between the critical temperature and the cricondentherm. The gas will drop out liquid by retrograde condensation in the reservoir, when the pressure falls below the dew point. This heavy part of the gas has found many application in industry and also in daily life and by remaining in reservoir not only this valuable liquid is lost but also its accumulation will result in forming a condensate bank near the well bore region which makes a considerable reduction in well productivity. This highlights the need to find an economical way to increase the condensate recovery from these reservoirs. Wells in gas condensate reservoirs usually exhibit complex behaviors due to condensate deposition as the bottom hole pressure drops below the dew point. Formation of this liquid saturation results in reduced gas relative permeability around the well bore and a loss of gas productivity. One of the several ways of minimizing the pressure drop in order to reduce liquid drop-out is hydraulic fracturing before or after the development of the condensate bank. The pressure transients are often used as a reliable evaluation of stimulation performance for field development planning. It has been shown that condensate deposits effects can be identified and quantified by well test analysis dealing with a well test composite behavior; which, in presence of hydraulic fractures becomes much more complex. But the various impacting factors of stimulation; such as fracture length, conductivity, orientation, etc. can also be observed and defined in these analyses. In this paper, modeling and interpretation of pressure transient responses of multiple hydraulic fractured horizontal wells using a numerical reservoir model has been investigated.

## 1 Introduction

The first step in studying the gas condensate reservoirs is to characterize the reservoir fluid. It has been found that characterization of the gas condensate fluid is strongly influenced by some main factors such as hold up of retrograde condensate in the formation resulting in excessive producing gas to liquid ratio (GLR). Figure 1 shows a common characteristic of gas condensate fluids. The liquid drop out reaches a maximum and then decreases by vaporization during pressure depletion. This behavior may imply that when the reservoir pressure decreases sufficiently, the condensate will be recovered by re-vaporization. However, by the time pressure falls below the dew point, the original

© The Author(s), under exclusive license to Springer Nature Singapore Pte Ltd. 2022

J. Lin (Ed.): IPPTC 2021, *Proceedings of the 2021 International Petroleum and Petrochemical Technology Conference*, pp. 13–27, 2022.

[https://doi.org/10.1007/978-981-16-9427-1\\_2](https://doi.org/10.1007/978-981-16-9427-1_2)

phase diagram is no longer valid as the system composition changes during the production period. The compositional analysis of gas condensate fluids is conducted generally in more details than that of oil. The compositional data are used often in phase behavior models, particularly in reservoir simulation. The fluid is commonly analyzed by flashing it at the atmospheric pressure and measuring the composition of the stabilized gas and liquid phases. The fluid heavy fraction is analyzed to identify major components, and also characterize it by extended carbon groups, as the results of phase behavior models are very sensitive to the heavy end description of gas condensate systems.

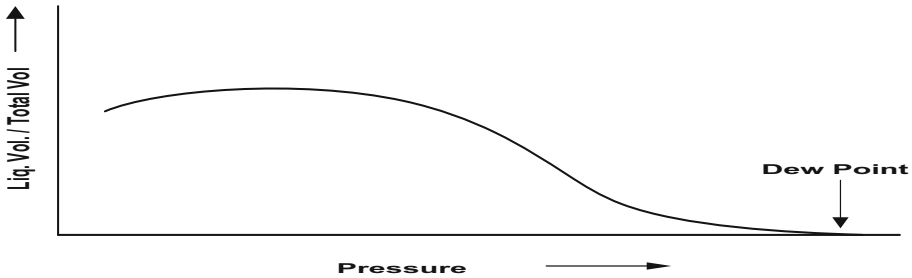


**Fig. 1.** Liquid drop out of gas condensate

Figure 2 shows pressure temperature relationship for gas condensate fluid with constant composition. Figure 3 shows effect of composition change on phase envelope.

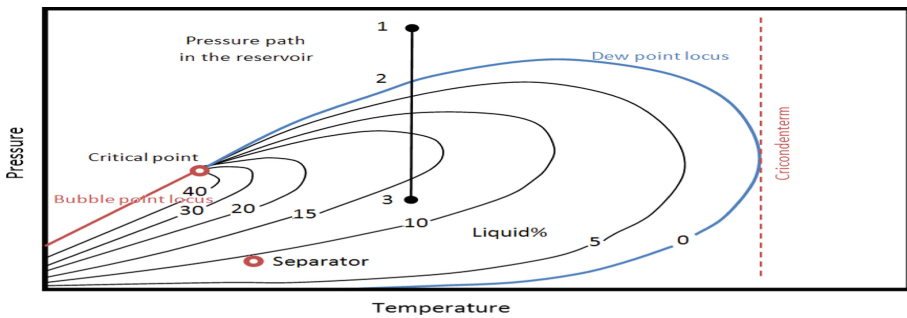


**Fig. 2.** Pressure – temperature curve for gas condensate with constant composition

In gas condensate reservoirs, gas injection and gas recycling are practices applied to reduce the drop out of the condensate in the reservoir. Gas injection can be implemented at the initial reservoir pressure to maintain the pressure above the dew point (full pressure maintenance), or after the reservoir pressure falls below the dew point (partial pressure maintenance) in which injection gas vaporizes the condensate and reduces the condensate accumulation in the reservoir. Gas recycling has been implemented in gas condensate reservoir for many years, but the increasing application of the reservoir gas and as a result its price made the engineers find an appropriate replace for it.  $N_2$  and  $CO_2$  were suggested



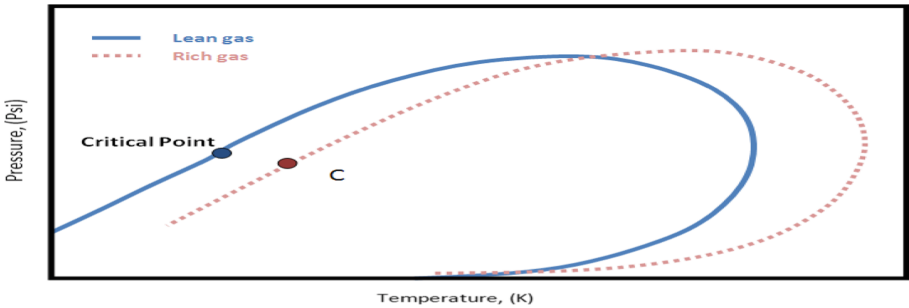


Fig. 3. Effect of composition change on phase envelope

as two alternatives which are now applied in some reservoirs. Nitrogen injection is not as effective as CH<sub>4</sub> and CO<sub>2</sub> injection, but as it is available and non-corrosive it can be properly applied for this purpose. Figure 4 shows condensate saturation in reservoir and Fig. 5 shows gas saturation versus relative permeability.

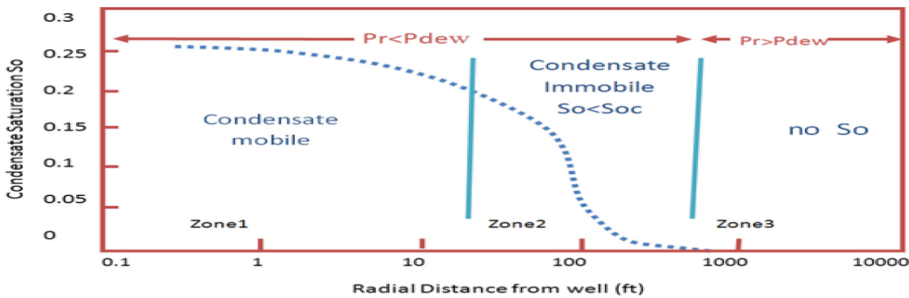


Fig. 4. Condensate saturation in reservoir

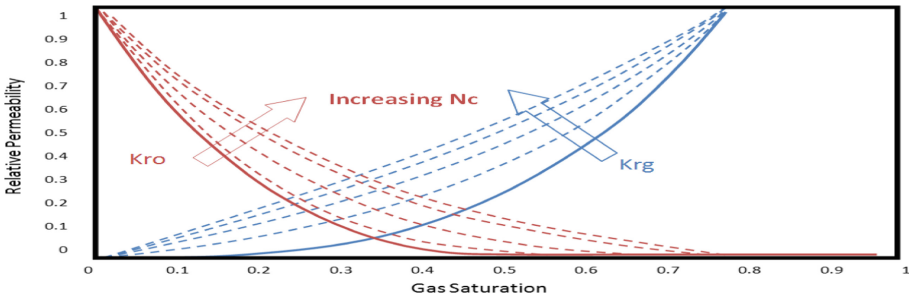


Fig. 5. Gas saturation versus relative permeability

## 2 Purpose of Study

This work investigates the modeling and interpretation of pressure transient response of multiple hydraulic fractured vertical wells in gas condensate reservoirs, using a fully compositional numerical reservoir model. After validating the numerical model using an analytical solution applied to a simpler reservoir/well model, complex reservoirs using the condensate PVT data are simulated and pressure transient response signatures obtained. Sensitivities of key reservoir/well/fracture properties are investigated and a result of each case is presented.

## 3 Methodology

The main aim of this investigation is to know fractured vertical wells behavior in a gas condensate reservoir. For this purpose, we use a compositional numerical model with one well to be able to predict derivative curves for fractured vertical wells with a pressure below dew point pressure. We use ECLIPSE 300 software which is compositional software. First, input data for numerical simulated model, fluids properties and initial reservoir parameters will be introduced. Then, three dimensional compositional models including one well with numbers of hydraulic fractures will be built. Finally, the results of this study will be discussed.

## 4 Cylindrical Compositional Model and Hydraulic Fracturing in Gas Condensate Reservoirs

Figure 6 shows a general pseudo- pressure logarithmic plot and its derivative plots for a vertical well in a two phase gas condensate reservoir. Figure 7 shows a fracture in a reservoir. Figure 8 shows effective well radius for a fracture with infinite conductivity. Figure 9 shows that slope 0.5 is a character for characterization fracture with infinite conductivity. Figure 10 shows that there is a little difference between steady state and non-steady state hydraulic fracture.

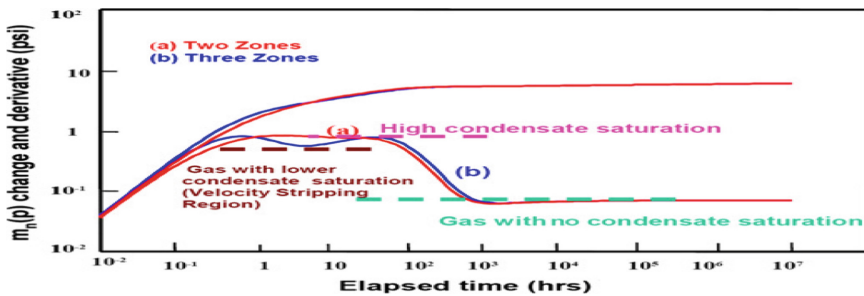


Fig. 6. Models for a well with two or three cylindrical compositional regions

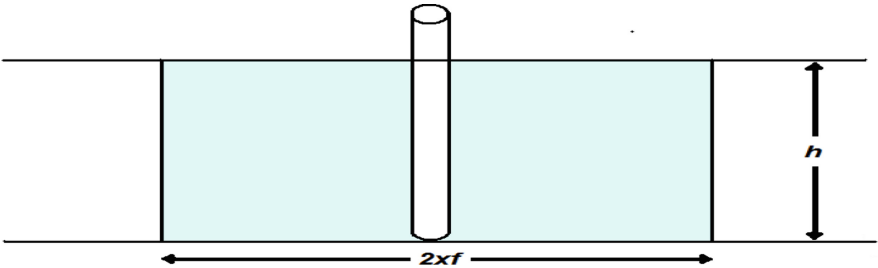


Fig. 7. Fracture in a reservoir

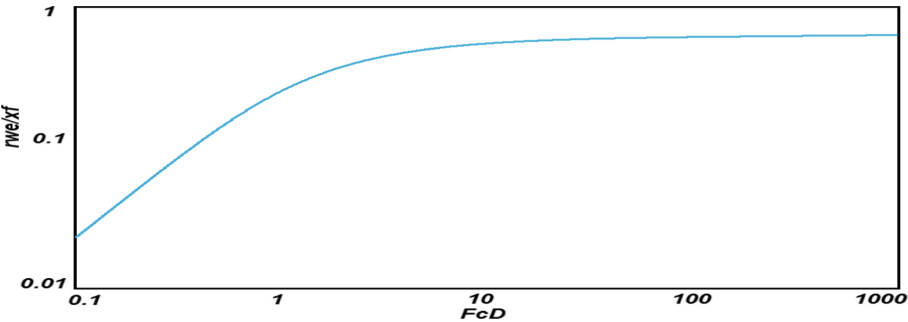


Fig. 8. Effective well radius for a fracture with infinite conductivity

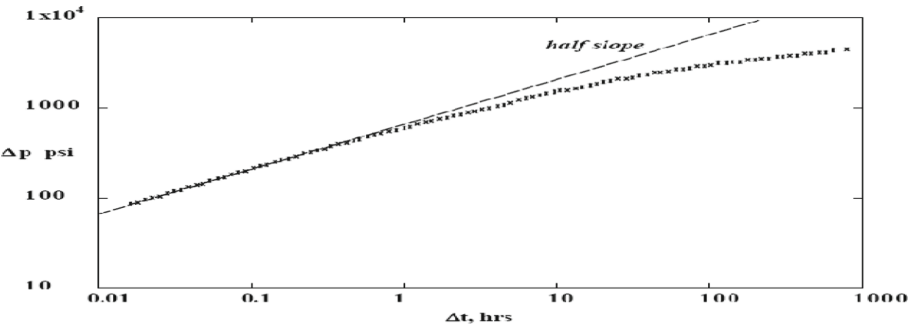
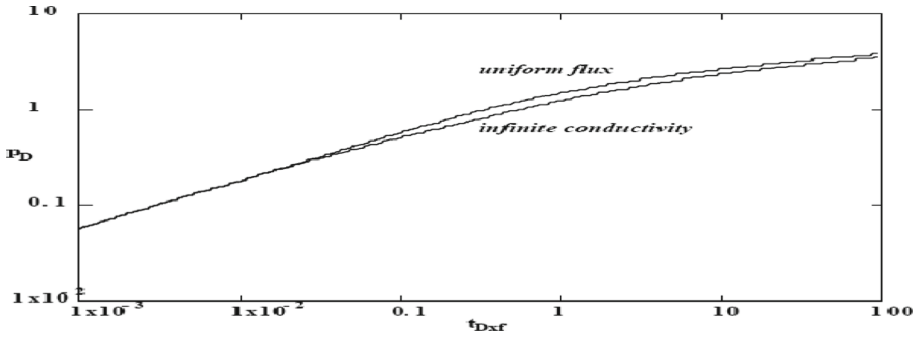


Fig. 9. Slope 0.5 is a character for characterization fracture with infinite conductivity



**Fig. 10.** A little difference between steady state and non-steady state hydraulic fracture

## 5 Fluid Properties Modeling

The main part of gas condensate reservoir modeling is finding a suitable fluid model. As fluid modeling and model optimization using laboratory data of fluid was not our purpose in this study, we use a prepared simulated fluid from a gas condensate reservoir and its properties as input data for simulation software. The composition of this fluid is shown in Table 1.

**Table 1.** Composition of fluid which was used in simulation

Mole%	Component	Number
0/0046	N <sub>2</sub>	1
0/0061	CO <sub>2</sub>	2
0/0	H <sub>2</sub> S	3
0/6864	C <sub>1</sub>	4
0/139	C <sub>2</sub>	5
0/0689	C <sub>3</sub>	6
0/0066	iC <sub>4</sub>	7
0/0266	nC <sub>4</sub>	8
0/0062	iC <sub>5</sub>	9
0/0094	nC <sub>5</sub>	10
0/014	C <sub>6</sub>	11
0/0348	C <sub>7</sub> +	12
Sum		1

## 6 Building Numerical Model for Simulation

A three dimensional model with one vertical well was built by ECLIPSE 300 software. For this simulation, we used a reservoir with thickness of 100 foot and length of 450 foot along Cartesian X-Y axes. In this model, we ignored wellbore storage effect and skin factor. Initial reservoir, rock and fluid properties are summarized in Table 2.

**Table 2.** Initial reservoir, rock and fluid properties which was used in model

Porosity	0.2
Initial water saturation	0.349
Well radius	0.3 foot
Isothermal rock compressibility coefficient	0.000004 1/psi
Total length of reservoir	17800 foot
Total width of reservoir	16100 foot
Horizontal permeability	10 md
Vertical permeability	1 md

## 7 Numerical Gridding Analyzing

Sizes of grids especially near well bore are very important because of its effects on fluid saturation and pressure of each block. Therefore, we must optimize lengths of grids in each direction. To do this, several model with different number of grids, 4669 ( $7 \times 23 \times 29$ ), 5887 ( $7 \times 29 \times 29$ ), 10933 ( $13 \times 29 \times 29$ ), 20787 ( $13 \times 39 \times 41$ ), and 31447 ( $13 \times 59 \times 41$ ) were tested. To study and understand gas condensate behavior near well bore clearly, we used small grid sizes around well bore and bigger grid sizes for grids which are far from well bore. Outer layers are selected with so big sizes that boundary effects on well test results can be ignored. The main purpose of selection this type of gridding was to be able to study flow regimes and accumulated condensate distribution during production or well test period more clearly and carefully. Finally, the model with 20787 ( $13 \times 39 \times 41$ ) was selected as the best model. Gridding system used for this model was shown in Fig. 11 and its grid sizes are shown in Table 3.

There are two methods to design grids sizes and grid refinement around well bore using ECLIPSE300 software which are Near Wellbore Module (NWM) and Template (Fig. 12).

One of the advantages of NWM model is that numbers of grids in a reservoir are less than a case which total reservoir is divided into smaller grids. But, as larger grids are located along side small grids, its calculation error will be increased. To use this model, first, that part of the reservoir which include well and hydraulic fractures must be departed from total reservoir, then, by selecting type of refined grids and based on local grid refinement theory, smaller grids around wellbore and fractures will be built.

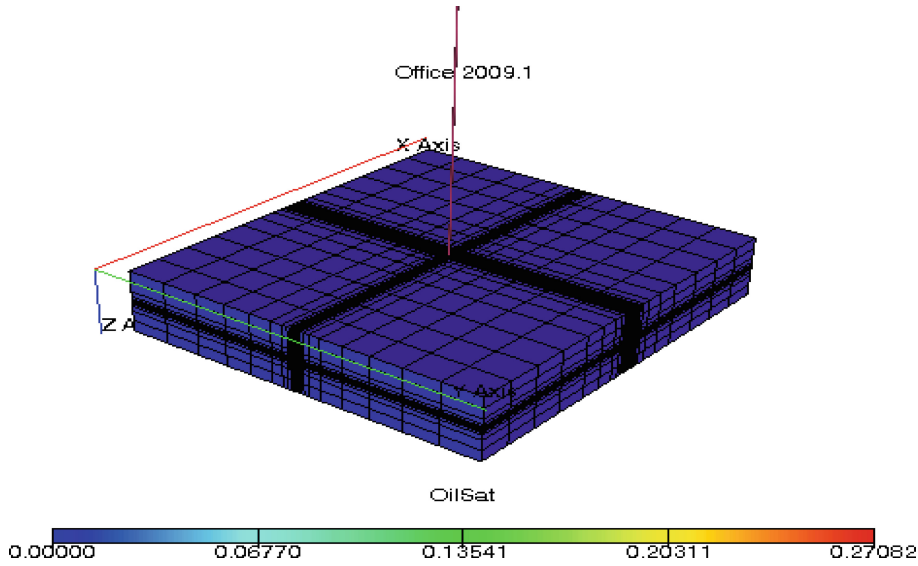


**Fig. 11.** Cartesian grid system for simulated model

**Table 3.** Grid sizes used for simulated model

$i$	$Dx$	$i$	$Dx$	$j$	$Dy$	$j$	$Dy$	$k$	$Dz$
1	1500	21	35	1	1500	21	0.25	1	17.8888
2	1500	22	35	2	1500	22	0.25	2	16
3	1500	23	35	3	1500	23	0.45	3	8
4	1500	24	35	4	1500	24	.8	4	4
5	1000	25	35	5	1014	25	1.4	5	2
6	800	62	35	6	512	62	2.5	6	2
7	400	27	35	7	256	27	5	7	1
8	200	28	35	8	128	28	10	8	2
9	88	29	35	9	64	29	20	9	2
10	45	30	35	10	35	30	35	10	4
11	35	31	45	11	20	31	64	11	8
12	35	32	88	12	10	32	128	12	16
13	35	33	200	13	5	33	256	13	17.88
14	35	34	400	14	2.5	34	512		
15	35	35	800	15	1.4	35	1014		
16	35	36	1000	16	0.8	36	1500		
17	35	37	1500	17	0.45	37	1500		
18	35	38	1500	18	0.25	38	1500		
19	35	39	1500	19	0.25	39	1500		
20	35	40	1500	20	0.25	40			